Low-altitude Aerial Color Digital Photographic Survey of the San Andreas Fault

David K. Lynch and Kenneth W. Hudnut
U.S. Geological Survey, Pasadena

David S. P. Dearborn
Lawrence Livermore National Laboratory

Online material: Images, navigation tools, GPS information for each image, web albums, flight path.

INTRODUCTION

Ever since 1858, when Gaspard-Félix Tournachon (pen name *Félix Nadar*) took the first aerial photograph (Professional Aerial Photographers Association 2009), the scientific value and popular appeal of such pictures have been widely recognized. Indeed, Nadar patented the idea of using aerial photographs in mapmaking and surveying. Since then, aerial imagery has flourished, eventually making the leap to space and to wavelengths outside the visible range. Yet until recently, the availability of such surveys has been limited to technical organizations with significant resources. Geolocation required extensive time and equipment, and distribution was costly and slow. While these situations still plague older surveys, modern digital photography and lidar systems acquire well-calibrated and easily shared imagery, although expensive, platform-specific software is sometimes still needed to manage and analyze the data. With current consumer-level electronics (cameras and computers) and broadband internet access, acquisition and distribution of large imaging data sets are now possible for virtually anyone.

In this paper we demonstrate a simple, low-cost means of obtaining useful aerial imagery by reporting two new, high-resolution, low-cost, color digital photographic surveys of selected portions of the San Andreas fault in California. All pictures are in standard jpeg format. The first set of imagery covers a 92-km-long section of the fault in Kern and San Luis Obispo counties and includes the entire Carrizo Plain. The second covers the region from Lake of the Woods to Cajon Pass in Kern, Los Angeles, and San Bernardino counties (151 km) and includes Lone Pine Canyon soon after the ground was largely denuded by the Sheep Fire of October 2009. The first survey produced a total of 1,454 oblique digital photographs (4,288 x 2,848 pixels, average 6 Mb each) and the second produced 3,762 nadir images from an elevation of approximately 150 m

above ground level (AGL) on the southeast leg and 300 m AGL on the northwest leg. Spatial resolution (pixel size or ground sample distance) is a few centimeters. Time and geographic coordinates of the aircraft were automatically written into the exchangeable image file format (EXIF) data within each jpeg photograph. A few hours after acquisition and validation, the photographs were uploaded to a publically accessible Web page. The goal was to obtain quick-turnaround, low-cost, high-resolution, overlapping, and contiguous imagery for use in planning field operations, and to provide imagery for a wide variety of land use and educational studies. This work was carried out in support of ongoing geological research on the San Andreas fault, but the technique is widely applicable beyond geology.

DATA ACQUISITION

Survey 1: Carrizo Plain and North to Choice Valley
On 24 September 2009 we carried out a systematic, low-altitude (~150 m AGL) aerial survey of a 91.8-km section of the San Andreas fault (SAF). Included were the entire Carrizo Plain starting south of CA-166/33 and sections north of CA-58 (Carissa Highway) up to the southern end of the Choice Valley (Figure 1). The main goal of this survey was to obtain high-resolution imagery of the section of the fault between highway CA-58 (Carissa Highway) and the southern end of the Choice Valley, approximately 29 km between ~N35 20 and N35 32. This region was chosen because it is generally inaccessible, and as a consequence has received far less attention than the Carrizo Plain to the southeast. Owing to the approach of the helicopter from the south, it was convenient to also acquire imagery of the SAF in the Carrizo Plain. All imagery was obtained at an elevation of approximately 150 m AGL.

The track was flown first northwest, immediately followed by a complementary southeast path. Both flight paths were offset from the trace by approximately 150 m NE and SW, producing oblique photographs and videos looking ~SW and ~NE respectively, with a line-of-sight dip angle of about 45 degrees. To enhance visibility of subtle topographic features, the flight
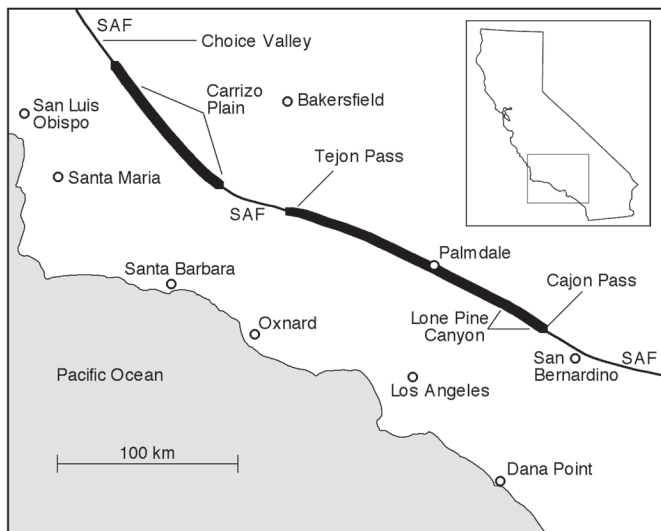
▲ **Figure 1.** Location Map. The main trace of the San Andreas fault (SAF) is shown as a thin black line and the two surveys reported here are indicated by thick black lines along the SAF.

was made when the sun was low in the sky. Imagery began at 16:03 PDT (sun elevation 33 degrees) and ended at 17:11 PDT (sun elevation 16 degrees). Average northwest and southeast flight speeds were 84 and 92 kts, respectively (43 & 47 m/s). The sky was cloud-free with unlimited visibility. Pictures were taken through open ports to avoid compromising image quality as might happen when shooting through glass or plastic windows. Navigation was based on pre-computed way points augmented by real-time corrections to optimize the imagery. Flight planning and trade-space optimization were carried out using FlightSim, spreadsheet-based software developed by the authors.

Imagery was obtained using a Nikon D90 digital single lens reflex camera with an attached GP-1 EXIF encoder. In all, 1,454 images were obtained, each with time, elevation, and geographic coordinates of the camera in the aircraft written into the image's EXIF file. Images were 4,288 × 2,848 pixels and the ground sample distance (GSD) of each center-of-frame pixel was approximately 4.2 cm, resulting in imagery with a spatial resolution (Nyquist sampling) of 8.4 cm. With a horizontal field of view (FOV) of 45 degrees, roughly 180 m, the picture to-picture overlap was about 30%, allowing easy correlation of adjacent images. Stereo pairs can also be extracted. Simultaneous high-definition MXP video (1,920 x 1,080 pixels) was obtained using a hand-held Canon HFS10 video camera, the width of whose images roughly matched those of the D90 camera.

Survey 2: Tejon Pass to Cajon Pass

The second survey was also a double-pass flight, this time with nadir-viewing geometry between Lake of the Woods (west of Tejon Pass) and Cajon Pass (Figure 1). Instead of viewing the ground obliquely from two different angles, we flew the first (southeast) leg at an elevation of roughly 150 m AGL and the return leg along the same flight path at about 300 m AGL. We

obtained a total of 3,762 images with GSDs of 4–8 cm. Survey 2 used the same photographic equipment from Survey 1 with the addition of a camera mount containing a remotely operated shutter release because the nadir port in the fixed-wing Partenavia was difficult to reach. This survey was also done "blind" in the sense that we could not see the ground, and we had to rely on the pilot's ability to fly the way points without real-time corrections to the flight path. The camera was in a fixed position and did not change its view angle as invariably would happen with a hand-held camera, resulting in a more consistently pointed set of images compared to Survey 1. Table 1 summarizes the circumstances of the two surveys.

One of the full frame images from Survey 1 is shown in Figure 2. Two pictures that reveal the level of detail in the photographs are presented in Figures 3 and 4. Images from Survey 1 can be found at http://www.sanandreasfault.org/ SAFCarrizo24Sep2009.html.

Those from Survey 2 (See "Approach to Future Surveys" below) can be found at http://www.sanandreasfault.org/ SAFMojave29Dec2009.html and in the electronic supplement to this paper.

As a service to the community, the photographs are public domain and carry no copyright. They may be freely downloaded and used by anyone for any purpose. We ask that people using the data include the acknowledgment "*USGS photograph by David K. Lynch, Kenneth W. Hudnut and David S. P. Dearborn (2009)*" and cite this paper.

DISCUSSION

Quick acquisition and dissemination of information remains a high priority for emergency responders. The surveys reported here demonstrate that digital imagery and the Internet combine to form a powerful tool for characterizing and planning mitigation strategies in emergencies. Less than six hours after Survey 1 was complete, the data were validated as to accuracy of EXIF information, quality of the imagery, and completeness relative to the goals of the flight. The full data set and some simple viewing tools were placed on a publicly accessible Web site less than 48 hours after the flight. Based on experience from Survey 1, the Survey 2 imagery was validated and placed on the Internet seven hours after the plane landed.

The surveys reported here document baseline surface conditions in the 2009 epoch. After future earthquakes or as civilization modifies the landscape, the pictures can be used to assess changes. Of particular interest is the Lone Pine Canyon area of Survey 2. In early October 2009, the Sheep Fire cleared most of the brush from the canyon and revealed many subtle fault landforms that have heretofore been shrouded by vegetation. Survey 2 was performed a few months after the fire and before the brush was able to regrow and obscure the ground.

Oblique images can be approximately though acceptably geolocated in a Google Earth 5.1 or later session (Figures 5A and B) and saved as kml/kmz files. The procedure involves overlaying a rectangular image on to the Google Earth imagery and then performing a bilinear stretch. This is done by

TABLE 1
Survey Summaries

Survey 1
24 September 2009, 1,454 oblique images (jpg), elevation ~150 m AGL
Carrizo Plain and north to Choice Valley, 92 km

	Start	End	Ground Sample Distance (GSD)
Track 1	N34.94747 W119.4181	N 35.53235 W120.0892	~4 cm variable
Track 2	N 35.53235 W120.0892	N34.92392 W119.3885	~4 cm variable

flight cost: $2,146.00 USD, Bell 206 B-III JetRanger helicopter

Survey 2
29 December 2009, 3,762 nadir images (jpg)
Tejon Pass (Lake of the Woods) to Cajon Pass, 151 km

|	Start	End	Ground Sample Distance (GSD)
Track 1	N34.81895 W118.9998	N34.26462 W117.4504	~4 cm, elevation ~150 m AGL
Track 2	N34.26159 W117.4441	N34.81954 W119.0045	~8 cm, elevation ~300 m AGL

flight cost: $1,556.00 USD, Partenavia P68-OBS fixed wing
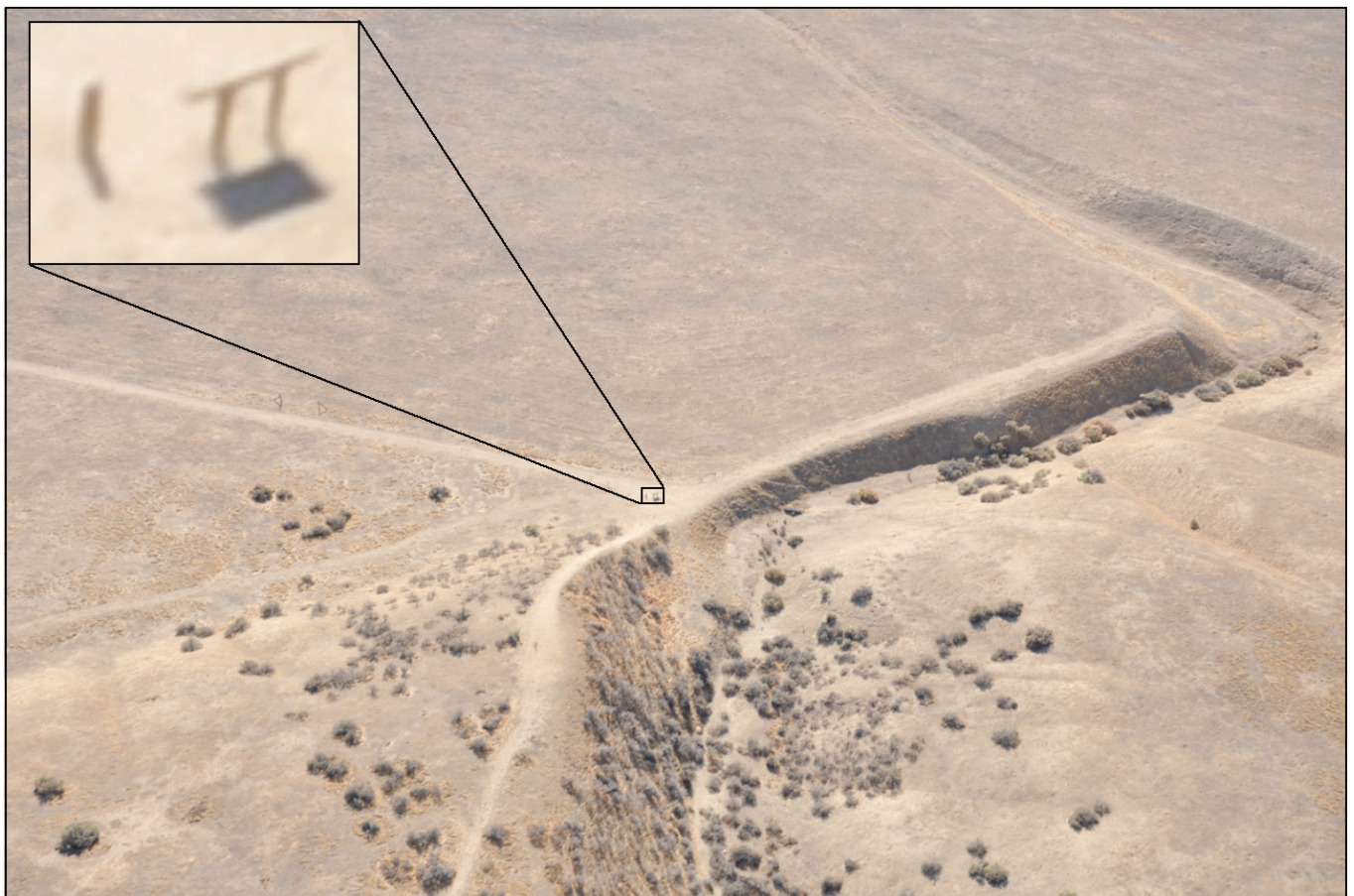
▲ **Figure 2.** Wallace Creek offset, looking NNW from an elevation of about 150 m AGL. The inset to the full frame shows a small post and a Carrizo Plain National Monument information sign, both about 0.8 m high. DSC_0373.

▲ **Figure 3.** Settlement on the SAF. Approximately 1/5 of the full frame from DSC_0403.
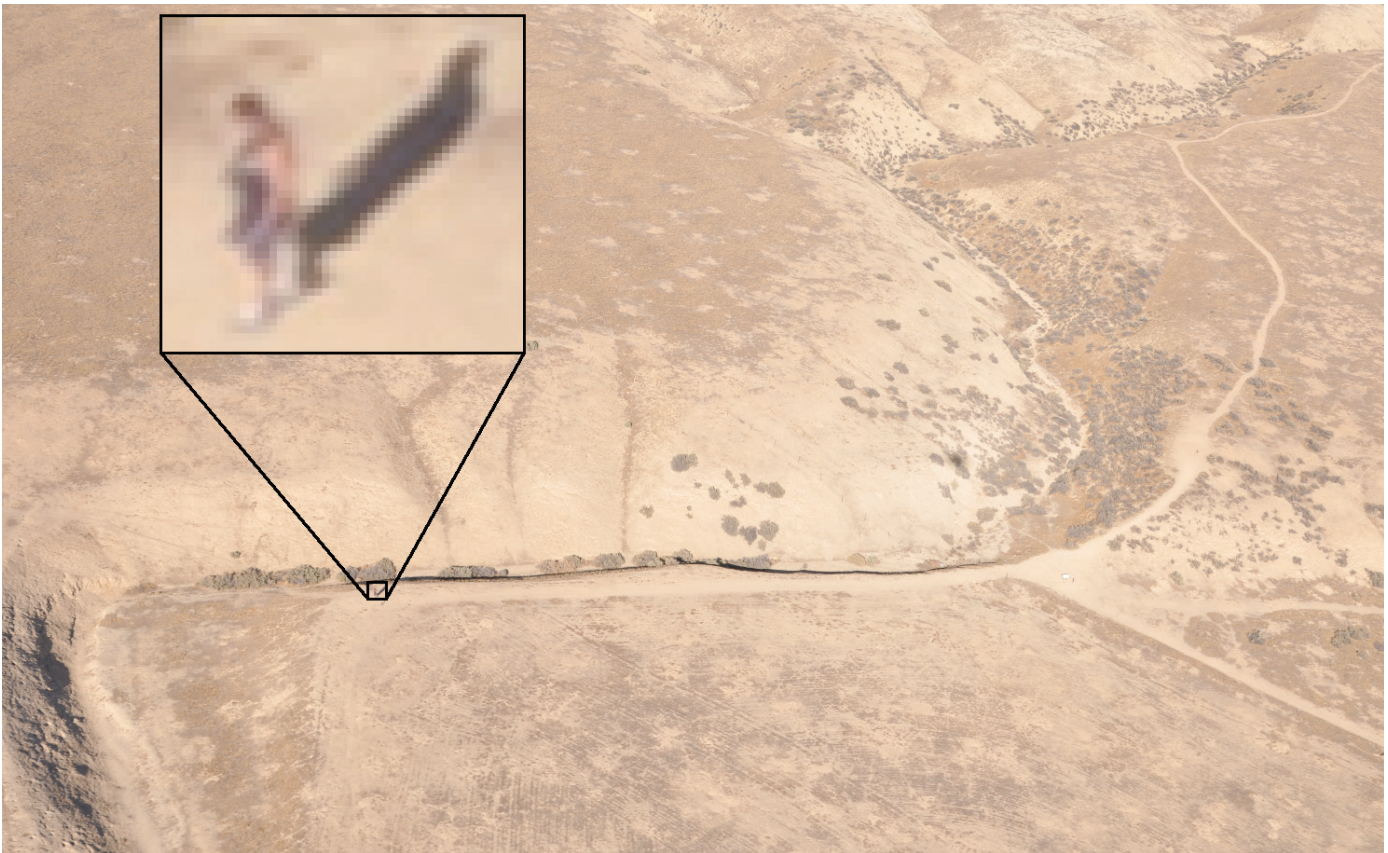
▲ **Figure 4.** Full frame image DSC_0974 of Wallace Creek. The inset shows a visitor. The pixel size at the center of the frame is about 4 cm.

hand, matching discrete terrain features such as bushes and road intersections. In Survey 1, features closest to the camera location (bottom of the camera image) appear to be geolocated to better than about one meter. Those farthest away (top of the image) are usually less accurately located. Since a bilinear stretch is applicable only to planar terrain, significant topography will result in systematic geolocation errors. Thus it is not as rigorous as more conventional techniques because each pixel in the stretched image does not carry geographic coordinates. This approach is tedious and does not produce a unique overlay. The results are nonetheless useful in correlating features on the ground because the stretched image retains its full resolution.

There is significant educational value in these color digital pictures. With free picture viewing software that is included in all personal computer operating systems, students can quickly scroll and zoom through the pictures to see a wide variety of geological features, including offset channels (Figure 2), scarps, pressure ridges, vegetation lineaments, landslides, beheaded channels, erosional features, and abandoned stream channels. Manmade features appear in many images (dirt tracks, houses, and fences, all resolved—see Figure 3). Thus users quickly gain an intuitive feel for the scale of things without the need for specialized software to compute and display scale bars. Students also see related features in context such as shutter ridges and offset channels, stepovers and grabens, sags and sag ponds, etc. The data set is homogeneous (obtained with the same equipment at nearly the same time), and navigation is simple because of overlap between successive images. Having the same region photographed from several different angles provides a 3D sense of the scene, and stereo pairs are easily extracted from both still imagery and HD video.

While the flights and imagery described here successfully demonstrated the concept of fast, inexpensive aerial surveys, a number of lessons were learned that are useful in executing future surveys.

1. Careful planning is required. We wrote a simple spreadsheet to calculate optimum flight speed, elevation, look angle, field of view, ground sample distance, picture interval, pixel size, image size, memory requirements, blurring due to aircraft motion, sun angle, flight cost and duration, etc. In preparing for low-altitude surveys, it is important to recognize the effect of topography: significant ground elevation changes result in variations in image scale and oblique view angle as the altitude AGL changes. For low altitude surveys (< 300 m AGL), image blurring along the flight direction can be a problem if the aircraft cannot fly slowly enough.

2. Precomputed way points and an aircraft/pilot who can fly them are essential. While much of the real-time navigation on Survey 1 was done by eye, when we lost sight of the fault or strayed from the planned track, we were quickly able to rejoin the planned route. A couple of short sections of the fault were missed on the southeast leg because we tried to navigate by eye and failed.

3. Holding cameras by hand for more than about 20 minutes is uncomfortable and leads to less than optimum pointing.

Therefore a system should be devised where the camera is suspended or cushioned to avoid vibrations and so the operator need only point the camera, not carry its entire weight. Tripods are unsuitable because they transmit aircraft vibration to the camera.

4. Back-up cameras, memory cards, and batteries should be readily accessible. While we did not need them this time, they were close by if necessary.

5. A dry run is mandatory, one in which pictures are taken in more or less the sequence that is planned. This verified that adequate storage space, battery life, and other operational requirements could be achieved. We even took the camera and GP-1 to the airport and confirmed their operation while the aircrafts' engines were running. This was necessary to ensure that the GPS signal could be received inside the shell of the aircraft and was not compromised by radiated electronic engine noise. We were pleasantly surprised to find that the GPS signal was strong inside both composite and metal aircraft skins, probably because of diffraction of the ~20-cm wavelength (1.57 GHz) GPS signal by the aircraft's windows.

6. During image acquisition using a hand-held camera, the intercoms should be set to "open" or "hot mike," because camera operators may not have a hand free to push the "talk" button for communication with the pilot. Reaching for the intercom and pushing the "talk" button might shift the operator's position and move the camera off target.

7. Oblique imaging poses different planning issues than does nadir imaging. Care must be taken to ensure that maximum image content is obtained, and this depends critically on the oblique view angle (Figure 6).

APPROACH TO FUTURE SURVEYS

Each researcher will have to decide what the best approach is for his or her surveys. However, based on the results of this flight, we have modified our baseline imaging plans to produce more useful imagery in the future. This revised approach is to fly two double-pass tracks on the same day using a nadir-pointing camera (Survey 2 was a test of this approach). The first double pass is done just after sunrise when the sun is between 10 and 20 degrees above the horizon, in order to reveal subtle ground topography. The first leg of the double pass is flown at low elevation—approximately 150 m AGL. The return leg follows the reverse ground track and is flown at much higher elevation (for example, ~600 m AGL) to include outlying topography and fault features that perhaps were not completely included in the low-elevation leg. The process is repeated the same day when the sun is setting and is again between 10 and 20 degrees above the horizon. This approach produces a homogeneous and essentially simultaneous data set consisting of four images of every location on the ground track from two different elevations and with two opposing sun angles.

When detection of subtle relief is desired, the duration of the imaging legs will be determined by the rate at which the sun altitude changes and how much the imaging team needs
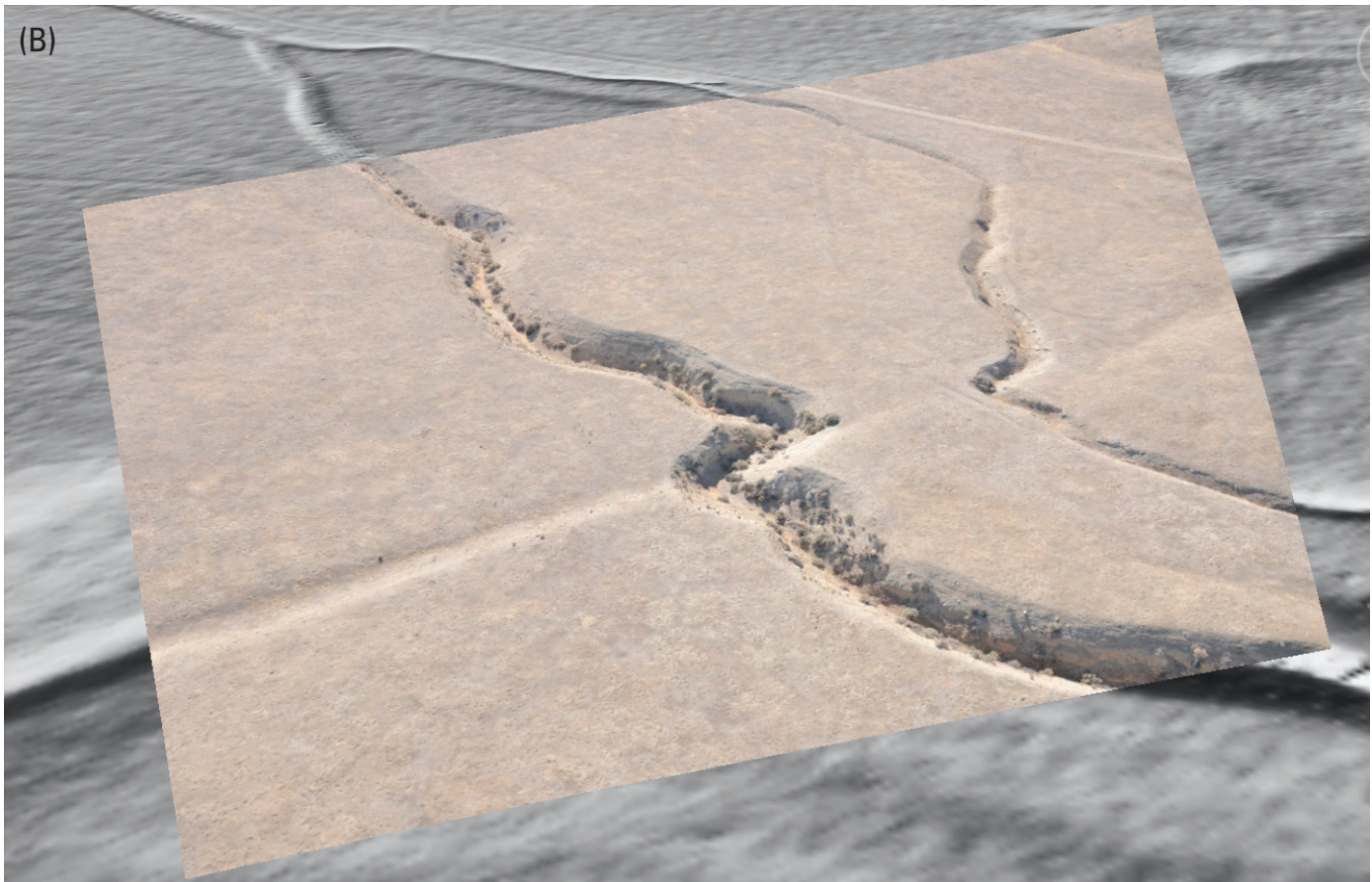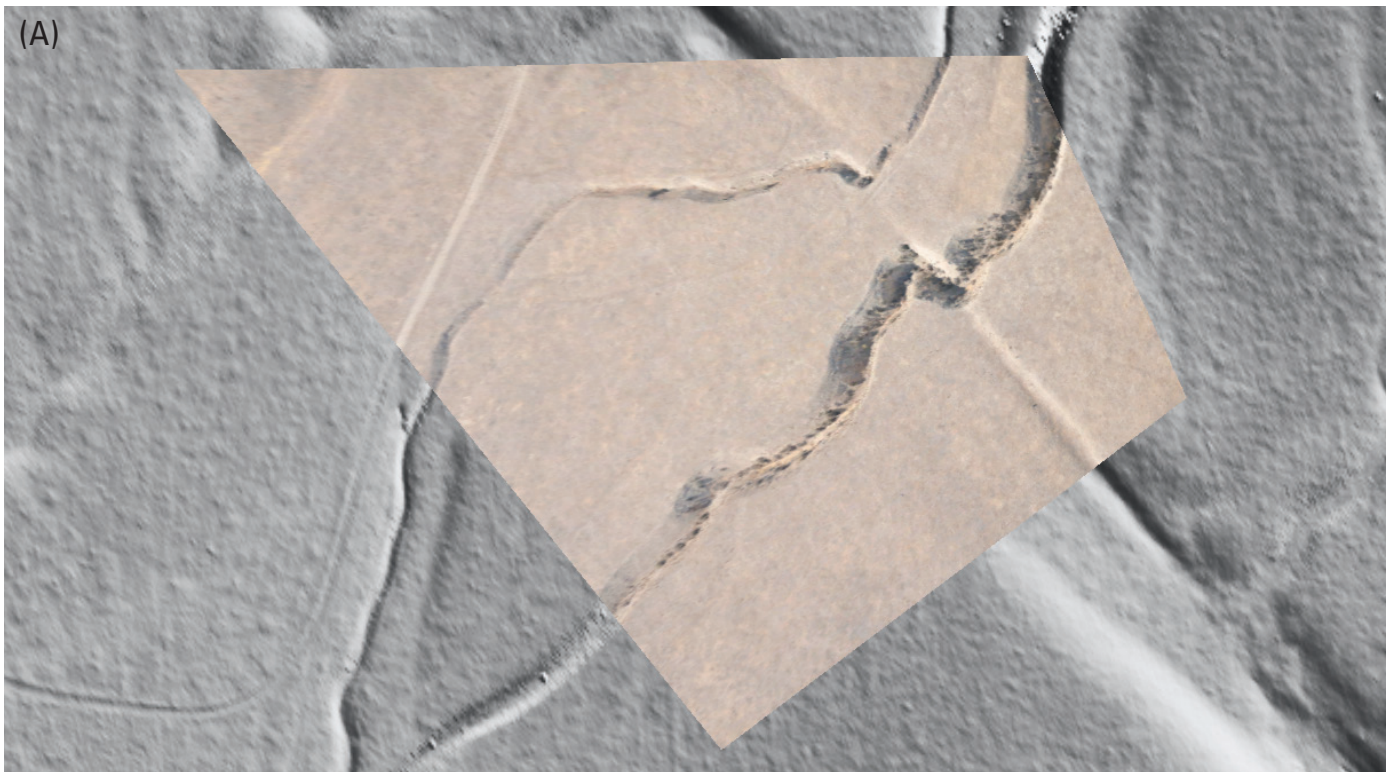
▲ Figure 5. A) Our image DSC_0385 has been distorted using a bilinear stretch function in Google Earth 5.1 and draped over the B4 lidar imagery (Bevis *et al.* 2005). B) Our image DSC_0385 image draped over the B4 imagery in an oblique view, representing the view from the aircraft.
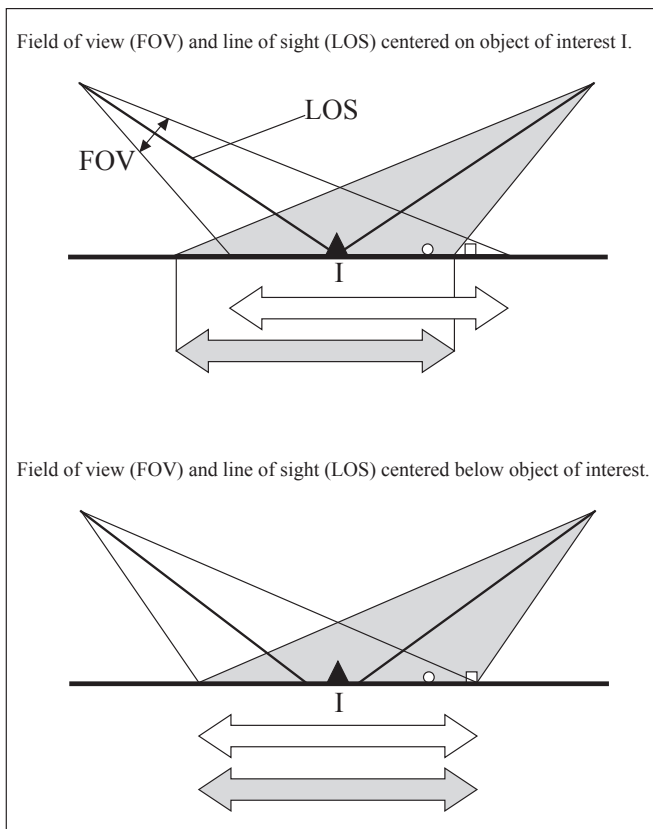
▲ Figure 6. Oblique imagery produces systematically biased ground coverage. This is important to consider on a double-pass flight when the goal is to image structures that are laterally (perpendicular to flight direction) equidistant from the object of interest (I). When the line-of sight (LOS) is centered on the object of interest, the edges of the top and bottom of the field of view (FOV) are not equal ground distances from center of the FOV; the top of the FOV is further from the object of interest than the bottom edge. In the case of a two-way oblique-imagery flight where images are desired from opposite directions, the ground coverage of the two views is not the same. To achieve identical ground coverages, the LOS must be below the object of interest by an angle that is easily calculated based on the geometry of the planned flight.

a limited sun angle. For example, at mid latitudes, the rising and setting sun elevation changes by approximately 1 degree every six minutes. Thus the sun is between 10 and 20 degrees altitude for about an hour, leading to a single-pass duration of 30 minutes. At a speed of 80 knots (41 m/s), a ground track approximately 74 km can be surveyed in 30 minutes.

SUMMARY AND CONCLUSIONS

We performed two quick-turnaround, low-cost color digital aerial surveys of the southern San Andreas fault and quickly placed the jpeg imagery on the Internet in the public domain.

Total cost was US$3,702, excluding the cost of the camera equipment. The 5,216 geolocatable pictures (~6 Mb each covering 243 km of the fault with a GSD of a few centimeters) were validated and made openly available within hours of acquisition. We outline an approach for doing future surveys and discuss logistical issues for aerial imagery. Such surveys are now possible at low cost using consumer-level cameras and widely available free software.

Postscript. The methods described have have become operational by USGS as part of its Haiti Earthquake Disaster Assistance Team (EDAT) geologic group's efforts to assess the threat of future earthquakes along the Enriquillo fault, and also to document the extensive surface ruptures along the Borrego fault and other faults in the Sierra El Mayor earthquake of northern Baja California. On Tuesday 6 April 2010 during helicopter reconnaissance of the extensive surface ruptures, Hudnut took more than 1,500 photos using this method. Also, while in Haiti nearly 10,000 photos were obtained in similar manner, although in Haiti there was very little surface faulting. ◣

ACKNOWLEDGMENTS

REFERENCES

Professional Aerial Photographers Association (2009); http://www.papainternational.org/history.html. Last accessed 31 March 2010.

Bevis, M., K. Hudnut, R. Sanchez, C. Toth, D. Grejner-Brzezinska, E. Kendrick, D. Caccamise, D. Raleigh, H. Zhou, S. Shan, W. Shindle, A. Yong, J. Harvey, A. Borsa, F. Ayoub, R. Shrestha, B. Carter, M. Sartori, D. Phillips, and F. Coloma (2005). The B4 Project: Scanning the San Andreas and San Jacinto fault zones. American Geophysical Union, Fall Meeting 2005, abstract #H34B-01; see also http://www.earthsciences.osu.edu/b4/Site/Welcome.html.

P.O. Box 953
Topanga, California 90290 U.S.A.
dave@caltech.edu
(D. K. L.)